Catalysis Letters Vol. 108, Nos. 1–2, April 2006 (© 2006)
DOI: 10.1007/s10562-006-0020-3

Catalytic activities of Al_2O_3-promoted $NiSO_4/TiO_2$ for acid catalysis

Jong Rack Sohn* and Jun Seob Lim

Department of Applied Chemistry, Engineering College, Kyungpook National University, Taegu 702-701, Korea

Received 15 September 2005; accepted 5 January 2006

A series of catalysts, $NiSO_4/Al_2O_3$–TiO_2, for acid catalysis was prepared by the impregnation method, where support, Al_2O_3–TiO_2 was prepared by the coprecipitation method using a mixed aqueous solution of titanium tetrachloride and aluminum nitrate solution followed by adding an aqueous ammonia solution. The addition of nickel sulfate (or Al_2O_3) to TiO_2 shifted the phase transition of TiO_2 from amorphous to anatase to higher temperature because of the interaction between nickel sulfate (or Al_2O_3) and TiO_2. 15-$NiSO_4$/5-Al_2O_3–TiO_2 containing 15 wt% $NiSO_4$ and 5 mol% Al_2O_3, and calcined at 400 °C exhibited maximum catalytic activities for both reactions, 2-propanol dehydration and cumene dealkylation. The catalytic activities for both reactions were correlated with the acidity of catalysts measured by the ammonia chemisorption method. The charge transfer from Ti atoms to the neighboring Al atoms strengthens the Al–O bond between Al and the surface sulfate species. The addition of Al_2O_3 up to 5 mol% enhanced the acidity, thermal property, and catalytic activities of $NiSO_4/Al_2O_3$–TiO_2 gradually due to the interaction between Al_2O_3 and TiO_2 and consequent formation ofAl–O–Ti bond.

KEY WORDS: $NiSO_4/Al_2O_3$–TiO_2; acidity, Al_2O_3-promotion; cumene dealkylation; 2-propanol dehydration.

1. Introduction

Acid catalysis is of fundamental industrial importance. Solid acid catalysts play on important role in hydrocarbon conversion reactions in the chemical and petroleum industries [1,2]. Liquid superacids based on HF, which are efficient and extensively used in catalytic processing, are not suitable for industrial processes due to separation problems tied with environmental regulations [3]. Many catalysts were reported in the literature including $AlCl_3$ with additives like $SbCl_3$ and HCl, chlorinated alumina, transition metal-exchanged zeolites, heteropoly acids, and some bifunctional catalysts [4]. Most of these catalysts suffer from different draw backs such as high working temperature, continuous supply of chlorine and a high-hydrogen pressure. Conventional industrial acid catalysts, such as sulfuric acid, $AlCl_3$, and BF_3, have unavoidable drawbacks because of their severe corrosivity and high susceptibility to water. Thus the search for environmentally benign heterogeneous catalysts has driven the worldwide research of new materials as a substitute for current liquid acids and halogen-based solid acids. Among them sulfated oxides, such as sulfated zirconia, titania, and iron oxide exhibiting high thermostability, superacidic property, and high catalytic activity, have evoked increasing interest [2,5,6]. The strong acidity of zircona-supported sulfate has attracted much attention because of its ability to catalyze many reactions such as cracking, alkylation, and isomerization.

* To whom correspondence should be addressed.
E-mail: jrsohn@knu.ac.kr

The concept that solid surfaces may be acidic arose from the observation that hydrocarbon reactions such as cracking that are catalyzed by acid-treated clays or silica alumina, give rise to a much different product distribution than those obtained by thermal reaction. These solid-catalyzed reactions exhibit features similar to reactions catalyzed by mineral acids. It is well known that the surface acidity of a metal oxide is improved with the incorporation of another metal oxide to form a mixed oxide catalyst. A number of combination of metal oxides generates acid sites [7–14]. TiO_2 alone is impractical as a catalyst because of its low catalytic activity. However, mixed oxide systems combining TiO_2 with such oxides as V_2O_5, MoO_3, P_2O_5, SiO_2, and ZnO are known to be effective for various reactions [15–18].

Recently, it has been found that a main group element Al can also promote the catalytic activity and stability of sulfated zirconia for *n*-butane isomerization [19,20]. The search for a more active catalyst is a never ending task. At the same time that increased catalytic activity is sought, an improvement in selectivity to the desired product is also required. Previously, it has been shown that nickel sulfate supported on TiO_2 is active for ethylene dimerization [21]. However, a major disadvantage associated with TiO_2 support is its low specific surface area and low thermal stability of the anatase structure at high temperatures. To overcome these deficiencies, titania was combined with Al_2O_3, by taking advantage of the high thermal stability and high surface area of Al_2O_3. In this paper, we report new catalyst system for acid catalysis, $NiSO_4/Al_2O_3$–TiO_2 prepared

by promoting TiO_2 with Al_2O_3 and supporting $NiSO_4$ to improve catalytic activity and thermal stability.

2. Experimental

2.1. Catalyst preparation

The Al_2O_3–TiO_2 mixed oxide was prepared by a co-precipitation method using aqueous ammonia as the precipitation reagent. The co-precipitate of $Al(OH)_3$–$Ti(OH)_4$ was obtained by adding aqueous ammonia slowly into a mixed aqueous solution of titanium tetrachloride and aluminum nitrate (Junsei Chemical Co.) at room temperature with stirring until the pH of the mother liquor reached about 8. Catalysts containing various nickel sulfate contents were prepared by the impregnation of $Al(OH)_3$–$Ti(OH)_4$ powder with an aqueous solution of $NiSO_4$, followed by calcining at different temperatures for 1.5 h in air. This series of catalysts is denoted by the mol percentage of Al_2O_3 and the weight percentage of nickel sulfate. For example, 15-$NiSO_4$/5-Al_2O_3–TiO_2 indicates the catalyst containing 5 mol% of Al_2O_3 and 15 wt% of $NiSO_4$.

2.2. Procedure

The FTIR spectra were obtained in a heatable gas cell at room temperature using a Mattson Model GL6030E spectrophotometer. The self-supporting catalyst wafers contained about 9 mg cm^{-2}. Prior to obtaining the spectra, we heated each sample under vacuum at 25–500 °C for 1 h. Catalysts were checked in order to determine the structure of the prepared catalysts by means of a Philips X'pert-APD X-ray diffractometer, employing Ni-filtered Cu K_α radiation. The DSC measurements were performed by a PL-STA model 1500H apparatus in air; the heating rate was 5 °C per minute. For each experiment 10–15 mg of sample was used.

The specific surface area was determined by applying the BET method to the adsorption of N_2 at −196 °C. Chemisorption of ammonia was also employed as a measure of the acidity of catalysts. The amount of chemisorption was determined based on the irreversible adsorption of ammonia [22–24].

2-propanol dehydration was carried out at 160–180 °C in a pulse micro-reactor connected to a gas chromatograph. Fresh catalyst in the reactor made of 1/4 in. stainless steel was pretreated at 400 °C for 1 h in a nitrogen atmosphere. Diethyleneglycol succinate on shimalite was used as packing material of the gas chromatograph and the column temperature for analyzing the product was 150 °C. Catalytic activity for 2-propanol dehydration was represented as mol of propylene converted from 2-propanol per gram of catalyst. Cumene dealkylation was carried out at 300–350 °C in the same reactor as above. Packing material for the gas chromatograph was Bentone 34 on chromosorb *W* and column temperature was 130 °C. Catalytic activity for cumene dealkylation was represented as mol of benzene converted from cumene per gram of catalyst. Conversions for both reactions were taken as the average of the first to sixth pulse values.

3. Results and Discussion

3.1. Infrared spectra

In general, for the metal oxides modified with sulfate ions followed by evacuation above 400 °C, a strong band assigned to S=O stretching frequency is observed at 1360–1410 cm^{-1} [25–27]. The infrared spectra of self-supported 15-$NiSO_4$/5-Al_2O_3–TiO_2 after evacuation at different temperatures for 1 h were examined. As shown in figure 1, there are sharp bands at 1358–1383 cm^{-1} accompanied by four broad but split bands at 1227, 1134, 1056, and 998 cm^{-1}, indicating the presence of two kinds of sulfated species. The bands at 1358–1383 cm^{-1} correspond to the asymmetric S=O stretching frequency of sulfate ion bonded to 5-Al_2O_3–TiO_2 under the dehydrated condition, while the latter four bands are assigned to bidentate sulfate ion coordinated to 5-Al_2O_3–TiO_2 [27,28]. Such results are very similar to those of other workers [26,28]. However, the frequency shift of this band is different depending on the evacuation temperature, as shown in figure 1. At 100 °C an asymmetric stretching band of S=O bonds was not

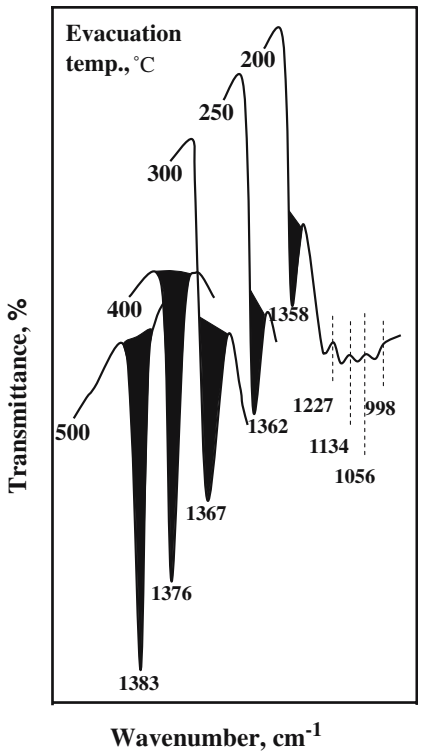

Figure 1. Infrared spectra of 15-$NiSO_4$/5-Al_2O_3–TiO_2 evacuated at different temperatures for 1h.

observed, because the water molecules are adsorbed on the surface of 15-$NiSO_4$/5-Al_2O_3–TiO_2 [27,28]. However, from 200 °C the band began to appear at 1358 cm^{-1}; the band intensity increased with the evacuation temperature and the position of band shifted to a higher wavenumber. That is, the higher the evacuation temperature, the larger the shift of the asymmetric stretching frequency of the S = O bonds. It is likely that the surface sulfur complexes formed by the interaction of oxides with sulfate ions in highly active catalysts have a strong tendency to reduce their bond order by the adsorption of basic molecules such as H_2O [27,28]. Consequently, as shown in figure 1, an asymmetric stretching band of S = O bonds for the sample evacuated at lower temperature appears at a lower frequency compared with that for the sample evacuated at higher temperature, because the adsorbed water reduces the bond order of S = O from a highly covalent double bond character to a lesser double bond character. We measured the acidity of 15-$NiSO_4$/5-Al_2O_3–TiO_2 evacuated at different temperatures by the chemisorption method of ammonia [22–24]. The acidity of the catalyst evacuated at 200, 300, 400, and 500 °C for 1 h was 198, 232, 301, and 313 μmol g^{-1}, respectively. Therefore, it is obvious that the asymmetric stretching frequencies of the S=O bonds are related to the acidic properties.

3.2. Crystalline structures of catalysts

The crystalline structures of catalysts calcined in air at different temperatures for 1.5 h were examined. In the case of titania support, as shown in figure 2, TiO_2 was amorphous to X-ray diffraction at 25 °C, with an anatase phase 300–400 °C, a two-phase mixture of the anatase and rutile forms at 500–600 °C, and a rutile phase at 700–800 °C. Three crystal structures of TiO_2, i.e., anatase, rutile, and brookite phases have been reported [29,30]. However, in the case of 5-Al_2O_3–TiO_2, the crystalline structures of the samples were different from the structure of pure TiO_2 (This figure is not shown here). 5-Al_2O_3–TiO_2 calcined at 400 °C are mostly amorphous. The transition temperature of TiO_2 from amorphous to anatase phase was higher by 200 °C than that of pure TiO_2. X-ray diffraction data indicated only the anatase phase of TiO_2 at 500–800 °C, showing that the amount of anatase TiO_2 phase increased with increasing the calcination temperature. It is assumed that the interaction between Al_2O_3 and TiO_2 hinders the phase transition of TiO_2 from amorphous to anatase [19,23,31].

The crystalline structures of 15-$NiSO_4$/5-Al_2O_3–TiO_2 calcined in air at different temperatures for 1.5 h were checked by X-ray diffraction. The 15-$NiSO_4$/5-Al_2O_3–TiO_2 materials calcined at different temperatures, as shown in figure 3, are mostly amorphous up to 500 °C. In other words, the transition temperature from amorphous to anatase phase was higher by 300 °C than that of pure TiO_2 [22]. X-ray diffraction data indicated only the anatase phase of TiO_2 at 500–800 °C, without detection of rutile TiO_2 phase. However, the amount of anatase TiO_2 phase increased with increasing the calcination temperature. It is assumed that the interaction between $NiSO_4$ (or Al_2O_3) and TiO_2 hinders the phase

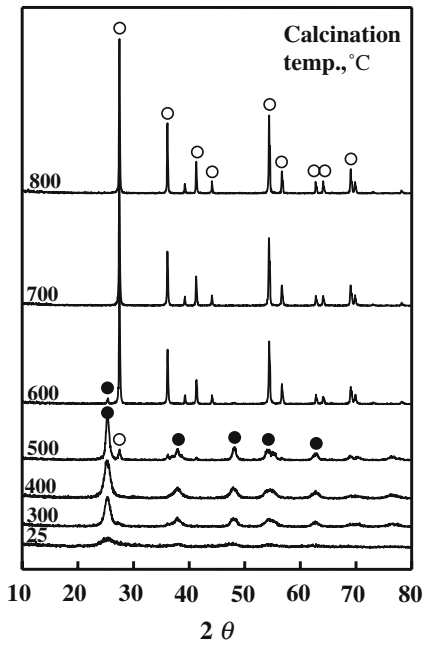

Figure 2. X-ray diffraction patterns of TiO_2 calcined at different temperatures for 1.5 h: (○), anatase phase of TiO_2. (●), rutitle phase of TiO_2.

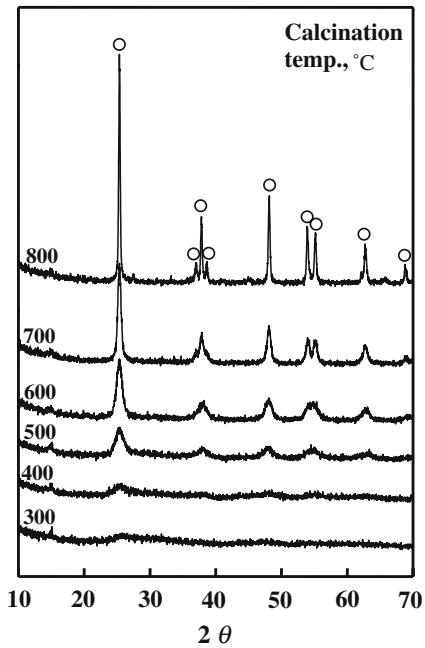

Figure 3. X-ray diffraction patterns of 15-$NiSO_4$/5-Al_2O_3–TiO_2 calcined at different temperatures for 1.5 h: (○), anatase phase of TiO_2.

transition of TiO_2 from amorphous to anatase [19,31]. For the above Al_2O_3-promoted catalysts, there are no characteristic peaks of Al_2O_3 in the patterns, implying that Al_2O_3 is sufficiently homogeneously mixed with titania.

3.3. Thermal analysis

The X-ray diffraction patterns in figures 2 and 3 clearly show that the structure of $NiSO_4/Al_2O_3$–TiO_2 is different depending on the calcined temperature. To examine the thermal properties of precursors for $NiSO_4/Al_2O_3$–TiO_2 samples more clearly, we completed their thermal analysis; the results are illustrated in figure 4. For pure TiO_2, the DSC curve shows a broad endothermic peak below 200 °C due to water elimination, and two exothermic peaks at 303 and 602 °C due to the phase transition of TiO_2 from amorphous to anatase, and from anatase to rutile, respectively [32]. However, it is of interest to see the influence of Al_2O_3 and $NiSO_4$ on the crystallization of TiO_2 from amorphous to anatase phase. As figure 4 shows, the exothermic peak due to the crystallization appears at 303 °C for pure TiO_2, while for 5-Al_2O_3–TiO_2 samples it is shifted to higher temperatures due to the interaction between Al_2O_3 and TiO_2. Consequently, the exothermic peak appear at 497 °C for 5-Al_2O_3–TiO_2.

However, for $NiSO_4$/5-Al_2O_3–TiO_2 samples containing different $NiSO_4$ contents, the DSC patterns are somewhat different from that of Al_2O_3–TiO_2. As shown in figure 4, the exothermic peak for $NiSO_4$/5-Al_2O_3–TiO_2 due to the crystallization of TiO_2 is shifted to higher temperatures compared with that for 5-Al_2O_3–TiO_2 without $NiSO_4$, indicating that there is an interaction between $NiSO_4$ and TiO_2 in addition to the interaction between Al_2O_3 and TiO_2. The shift increases with increasing $NiSO_4$ content. The endothermic peaks at 764 °C for $NiSO_4/Al_2O_3$–TiO_2 samples are due to the evolution of SO_3 decomposed from sulfate species bonded to the surface of Al_2O_3–TiO_2 [19,33]. For pure $NiSO_4 \cdot 6H_2O$, the DSC curve shows three endothermic peaks below 400 °C due to water elimination, indicating that the dehydration of $NiSO_4 \cdot 6H_2O$ occurs in three steps. The endothermic peak around 837 °C is due to the evolution of SO_3 decomposed from nickel sulfate [19,33]. Decomposition of nickel sulfate is known to begin at 700 °C [34].

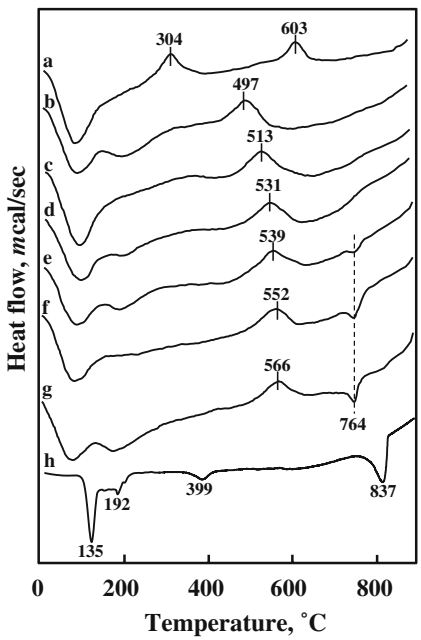

Figure 4. DSC curves of $NiSO_4$/5-Al_2O_3–TiO_2 precursors having different $NiSO_4$ contents: (a) TiO_2, (b) 5-Al_2O_3–TiO_2, (c) 3-$NiSO_4$/5-Al_2O_3–TiO_2, (d) 5-$NiSO_4$/5-Al_2O_3–TiO_2, (e) 10-$NiSO_4$/5-Al_2O_3–TiO_2, (f) 15-$NiSO_4$/5-Al_2O_3–TiO_2, (g) 20-$NiSO_4$/5-Al_2O_3–TiO_2, and (h) $NiSO_4 \cdot xH_2O$.

3.4. Surface properties

The specific surface areas of $NiSO_4$/5-Al_2O_3–TiO_2 catalysts containing different $NiSO_4$ contents and calcined at 400 °C for 1.5 h are listed in table 1. The presence of nickel sulfate and Al_2O_3 influences the surface area in comparison with that of the pure TiO_2. Specific surface areas of $NiSO_4$/5-Al_2O_3–TiO_2 samples are larger than that of 5-Al_2O_3–TiO_2 calcined at the same temperature, showing that surface area increases gradually with increasing nickel sulfate loading up to 15 wt%. It seems likely that the interactions between nickel sulfate (or Al_2O_3) and TiO_2 prevent catalysts from crystallizing [35]. The decrease of surface area for $NiSO_4$/5-Al_2O_3–TiO_2 samples containing $NiSO_4$ above 15 wt% is due to the blocking of TiO_2 pores by the increased $NiSO_4$ loading. The acidity of catalysts calcined at 400 °C, as determined by the amount of NH_3 irreversibly adsorbed at 230 °C [21–23], is also listed in table 1. The variation of acidity runs parallel to the change of surface area. The acidity increases with increasing nickel sulfate content up to 15 wt% of $NiSO_4$. The acidity is correlated with the catalytic activities for acid catalysis discussed below. We examined the effect of Al_2O_3 addition on the surface area and acidity of $NiSO_4/Al_2O_3$–TiO_2 samples. The specific surface areas and acidity of 15-$NiSO_4/Al_2O_3$-TiO_2 catalysts containing different Al_2O_3 contents and calcined at 400 °C are listed in table 2. Both surface area and acidity increased with increasing Al_2O_3 content up to 5 mol%, indicating the promoting effect of Al_2O_3 on the catalytic activities for acid catalysis described later.

Infrared spectroscopic studies of ammonia adsorbed on solid surfaces have made it possible to distinguish between Brönsted and Lewis acid sites [6,33,36,]. Figure 5 shows the infrared spectra of ammonia adsorbed on 15-$NiSO_4$/5-Al_2O_3–TiO_2 samples evacuated at 500 °C for 1 h. For 15-$NiSO_4$/5-Al_2O_3–TiO_2, the band at 1442 cm^{-1} is the characteristic peak of ammonium ion,

Table 1
Surface area and acidity of $NiSO_4/5\text{-}Al_2O_3$–TiO_2 catalysts containing different $NiSO_4$ contents and calcined at 400°C for 1.5 h

$NiSO_4$ content (mol%)	Surface area ($m^2\ g^{-1}$)	Acidity ($\mu mol\ g^{-1}$)
0	93	180
3	277	216
5	278	231
10	283	252
15	290	301
20	260	232

Table 2
Surface area and acidity of $15\text{-}NiSO_4/Al_2O_3$–TiO_2 catalysts containing different Al_2O_3 contents and calcined at 400 °C for 1.5 h

Al_2O_3 content (mol%)	Surface area (m^2/g^{-1})	Acidity ($\mu mol/g^{-1}$)
0	158	261
1	195	265
3	214	298
5	290	301
7	278	292
10	243	267

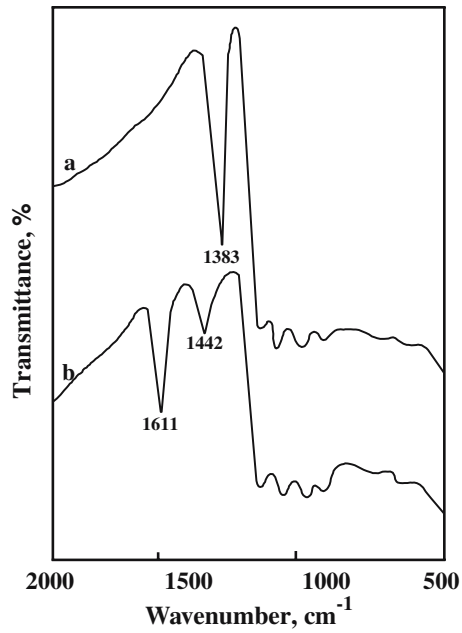

Figure 5. Infrared spectra of NH_3 adsorbed on $15\text{-}NiSO_4/5\text{-}Al_2O_3$–$TiO_2$: (a) background of $15\text{-}NiSO_4/5\text{-}Al_2O_3$–$TiO_2$ after evacuation at 500 °C for 1 h, (b) NH_3 adsorbed on (a), where gas was evacuated at 230 °C for 1 h.

which is formed on the Brönsted acid sites. The absorption peak at 1611 cm^{-1} is contributed by ammonia coordinately bonded to Lewis acid sites [6,33,36,], indicating the presence of both Brönsted and Lewis acid sites on the surface of $15\text{-}NiSO_4/5\text{-}Al_2O_3$–$TiO_2$ sample. Other samples having different nickel sulfate contents also showed the presence of both Lewis and Brönsted acids. As figure 5(a) shows, the intense band at 1383 cm^{-1} after evacuation at 500 °C is assigned to the asymmetric stretching vibration of S=O bonds having a high double bond nature [27,33]. However, the drastic shift of the infrared band from 1383 cm^{-1} to a lower wavenumber(not shown due to the overlaps of skeletal vibration bands of Al_2O_3–TiO_2) after ammonia adsorption[figure 5(b)] indicates a strong interaction between an adsorbed ammonia molecule and the surface complex. Namely, the surface sulfur compound in the highly acidic catalysts has a strong tendency to reduce the bond order of S=O from a highly covalent double-bond character to a lesser double-bond character when a basic ammonia molecule is adsorbed on the catalysts [27,33].

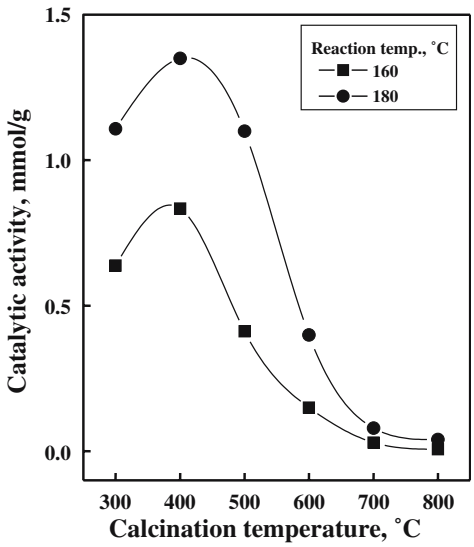

Figure 6. Catalytic activities of $15\text{-}NiSO_4/5\text{-}Al_2O_3$–$TiO_2$ for 2-propanol dehydration as a function of calcination temperature.

3.5. Catalytic activities for acid catalysis

3.5.1. Catalytic activities for 2-propanol dehydration and cumene dealkylation

Catalytic activities of $15\text{-}NiSO_4/5\text{-}Al_2O_3$–$TiO_2$ for 2-propanol dehydration and cumene dealkylation are plotted as a function of calcination temperature in figures 6 and 7, respectively. The activities for both reactions increased with the calcination temperature, reaching a maximum at 400 °C, after which the activities decreased. The decrease of activities for both reactions above 400 °C can be attributed to the fact that the surface area and acidity above 400 °C decrease with the calcination temperature. In fact, both surface area and acidity of $15\text{-}NiSO_4/5\text{-}Al_2O_3$–

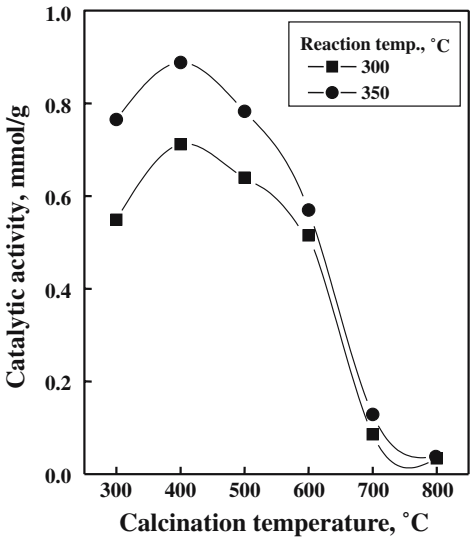

Figure 7. Catalytic activities of 15-$NiSO_4$/5-Al_2O_3–TiO_2 for cumene dealkylation as a function of calcination temperature.

TiO_2 above 400 °C were found to be decreased with the calcination temperature.

It is interesting to examine how catalytic activity of acid catalyst depends on the acid property. The catalytic activity for the 2-propanol dehydration was measured; the results are illustrated as a function of $NiSO_4$ content in figure 8, where the reaction temperature is 160–180 °C. In view of table 1 and figure 8, the variation in catalytic activity for 2-propanol dehydration can be correlated with the changes of their acid amount, showing the highest activity and acidity for 15-$NiSO_4$/5-Al_2O_3–TiO_2. It has been known that 2-propanol dehydration takes place very readily on weak acid sites [6,37]. Good correlations have been found in many cases between the acidity and the catalytic activities of solid acids. For example, the rates of both the catalytic decomposition of cumene and the polymerization of propylene over SiO_2–Al_2O_3 catalysts were found to increase with increasing acid amounts at strength $H_0 \leq +3.3$ [38]. It was also reported that the catalytic activity of nickel silicates in the ethylene demerization as well as in the butene isomerization was closely correlated with the acid amount of the catalyst [33,39].

Cumene dealkylation takes place on relatively strong acid sites of the catalysts [25,33,37]. Catalytic activities for cumene dealkylation against $NiSO_4$ content are presented in figure 9, where reaction temperature is 300–350 °C. It is confirmed that the catalytic activity gives a maximum at 15 wt% of $NiSO_4$. This seems to be closely correlated to the specific surface area and acidity of catalysts. As listed in table 1, both BET surface area and acidity attained a maximum extent when the $NiSO_4$ content in the catalyst was 15 wt% and then showed a gradual decrease with increasing $NiSO_4$ content. The correlation between catalytic activity and acidity holds for both reactions, 2-propanol dehydration and cumene dealkylation, although the acid strength required to catalyze acid reaction is different depending on the type of reactions. As seen in figures 8 and 9, the catalytic activity for cumene dealkylation, in spite of higher reaction temperature, is lower than that for 2-propanol dehydration.

3.5.2. *Effect of Al_2O_3 addition on catalytic activities*

The catalytic activities of 15-$NiSO_4$/Al_2O_3–TiO_2 as a function of Al_2O_3 content for the reaction of 2-propanol dehydration and cumene dealkylation were examined,

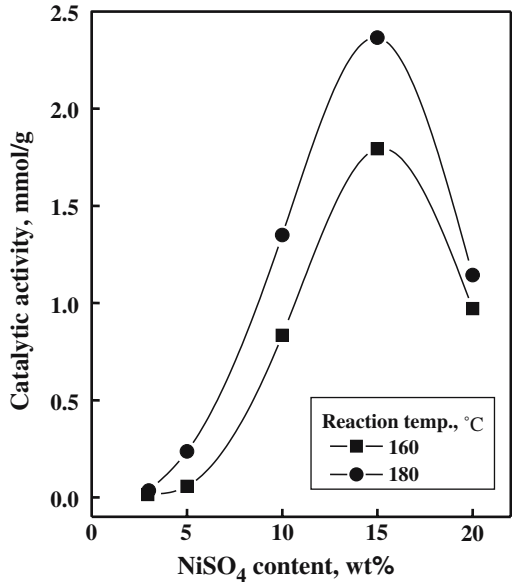

Figure 8. Catalytic activities of $NiSO_4$/5-Al_2O_3–TiO_2 for 2-propanol dehydration as a function of $NiSO_4$ content.

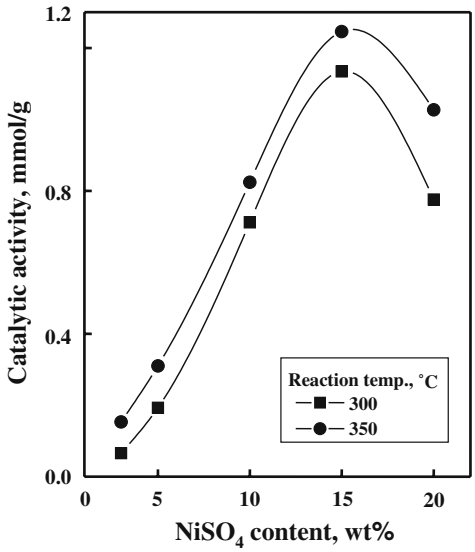

Figure 9. Catalytic activities of $NiSO_4$/5-Al_2O_3–TiO_2 for cumene dealkylation as a function of $NiSO_4$ content.

where the catalysts were pretreated at 400 °C for 1 h before reaction; the results are shown in the figures 10 and 11. The catalytic activities for both reactions increased with increasing the Al_2O_3 content, reaching a maximum at 5 mol%.

Considering the experimental results of table 2, and figures 10 and 11, it seems likely that the catalytic activities for both reactions closely relates to the change of acidity of catalysts. As listed in table 2, the total acid sites of 15-$NiSO_4$/5-Al_2O_3–TiO_2 and 15-$NiSO_4/TiO_2$ are 301μmol/g and 261μmol g^{-1}, respectively, showing that the number of acid sites for the catalyst promoted with Al_2O_3 is greater than that for nonpromoted catalyst. This is consistent with the results reported by Hua et al. over Al_2O_3-promoted SO_4^{2-}/ZrO_2 [19]. Al_2O_3-promoted catalysts could be related to a strong interaction between Al_2O_3 and TiO_2. Since the promoting effect of Al_2O_3 is related to an increase in number of surface acidic sites, it would be of interest to examine various factors influencing the enhancement of these surface acidic sites.

Xia et al. [40] proposed that Al_2O_3 incorporation in TiO_2 matrix brought about an increase of the positive partial charge on the Ti cations as a result of the formation of Al–O–Ti bonds which helped to stabilize the sulfate species at the oxide surface. The formation ofAl–O–Ti bond on the surface of the Al_2O_3-promoted catalysts is probably the cause for the increase in strong acidic sites. According to the principle of electronegativity equalization proposed by Sanderson [41], since the electronegativity of Al^{3+} is larger than that of Ti^{4+}, the positive charge on Ti atom is increased as a result of the formation ofAl–O–Ti bond, which generates stronger acidity on these sites [19]. At the same time, the

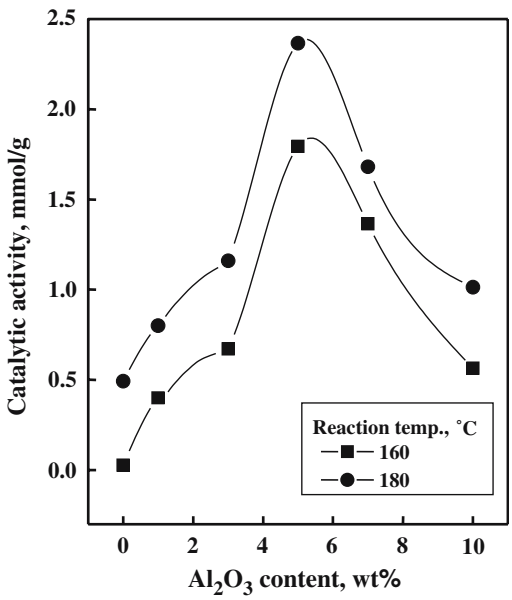

Figure 10. Effect of Al_2O_3 addition on catalytic activities of 15-$NiSO_4$/Al_2O_3–TiO_2 for 2-propanol dehydration.

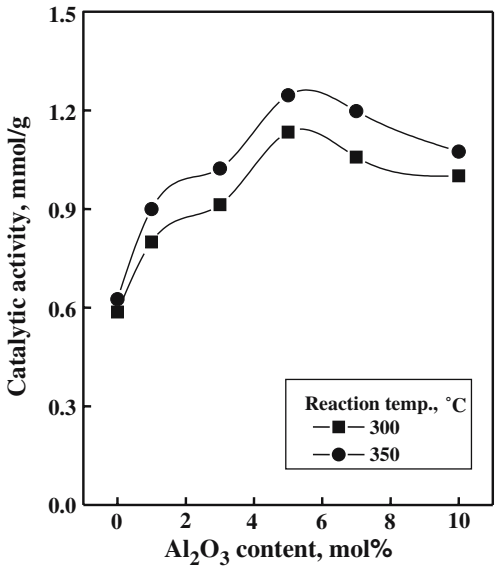

Figure 11. Effect of Al_2O_3 addition on catalytic activities of 15-$NiSO_4$/Al_2O_3–TiO_2 for cumene dealkylation.

strongerAl–O–Ti bond formed by the charge transfer from Ti atom to neighboring Al atom results in an increase in the thermal stability of the surface sulfate species and consequently the acidity of Al_2O_3-promoted catalyst is increased. In fact, to examine the thermal stability of the surface sulfate species DSC measurements were carried out. The endothermic peak due to the evolution of SO_3 decomposed from sulfate species bonded to the surface of TiO_2 appeared at 734 °C, while that from sulfate species bonded to the surface of Al_2O_3-promoted TiO_2 appeared at 768 °C. Such a temperature difference has been attributed to the stabilizing effect of the Al_2O_3 promoter on the sulfate species. Namely, the charge transfer from Ti atoms to the neighboring Al atoms strengthens the Al–O bond between Al and the surface sulfate species. The stronger Al–O bond leads to an increase in the thermal stability of the surface sulfate species and consequently the acidity of the catalysts is increased. A similar result was related by Gao et al.[42] to strong acid sites with differential heat of ammonia adsorption above 140 kJ mol^{-1}.

4. Conclusions

A series of catalysts, $NiSO_4/Al_2O_3$–TiO_2, were prepared by the impregnation method using an aqueous solution of nickel sulfate. The addition of nickel sulfate (or Al_2O_3) to TiO_2 shifted the phase transition of TiO_2 from amorphous to anatase to higher temperatures because of the interaction between nickel sulfate (or Al_2O_3) and TiO_2. 15-$NiSO_4$/5-Al_2O_3–TiO_2 containing 15 wt% $NiSO_4$ and 5 mol% Al_2O_3, and calcined at 400 °C, exhibited maximum catalytic activities for 2-propanol dehydration and cumene dealkylation. The

catalytic activity was correlated with the acidity of catalysts measured by the ammonia chemisorption method. The addition of Al_2O_3 up to 5 mol% enhanced the acidity, surface area, thermal properties, and catalytic activities of $NiSO_4/Al_2O_3$–TiO_2 for acid catalysis gradually, due to the interaction between Al_2O_3 and TiO_2 and due to consequent formation of Al–O–Ti bond.

Acknowledgments

This work was supported by the Brain Korea 21 Project in 2003. We wish to thank Korea Basic Science Institute (Daegu Branch) for the use of X-ray diffractometer.

References

[1] T.K. Cheung, J.L. d'Itri, F.C. Lange and B.C. Gates, Catal. Lett. 31 (1995) 153.
[2] K. Tanabe, M. Misono, Y. Ono and H. Hattori, *H, New Solid Acids and Bases* (Kodansha-Elsevier, Tokyo, 1989) 185.
[3] G.A. Olah, G.K.S. Prakash and J. Sommer, *Superacids* (Wiley-Interscience, New York, USA, 1985) 33–52.
[4] Y. Ono, Catal. Today 81 (2003) 3.
[5] K. Arata, Adv. Catal. 37 (1990) 165.
[6] J.R. Sohn and S.H. Lee, Appl. Catal. A: Gen. 266 (2004) 89.
[7] H.J.M. Bosman, E.C. Kruissink, J. van der Spoel and F. van der Brink, J. Catal. 148 (1994) 660.
[8] R.J. Davis and Z. Liu, Chem. Mater. 9 (1997) 2311.
[9] J.R. Sohn and H.J. Jang, J. Catal. 132 (1991) 563.
[10] I.J. Doh, Y.I. Pae and J.R. Sohn, J. Ind. Eng. Chem. 5 (1991) 161.
[11] J. Fung and I. Wang, J. Catal. 164 (1996) 166.
[12] G.M. Maksimov, M.A. Fedotov, S.V. Bogdanov, G.S. Litvak, A.V. Golovin and V.A. Likholobov, J. Mol. Catal. A:Chemical 158 (2000) 435.
[13] C. Contescu, V.T. Popa, J.B. Miller, E.I. Ko and J.A. Schwarz, Chem. Eng. J. 64 (1996) 265.
[14] M. Scheithauer, R.K. Grasselli and H. Knözinger, Langmuir 14 (1998) 3019.
[15] D.J. Hucknall, *Selective Oxidation of Hydrocarbons* (Academic Press, London/New York, 1974).
[16] M. Itoh, H. Hattori and K. Tanabe, J. Catal. 35 (1974) 225.
[17] K. Tanabe, G. Ishiya, I. Ichikawa and H. Hattori, Bull. Chem. Soc. Jpn. 45 (1972) 47.
[18] E.T.C. Vogt, A. Boot, A.J. Van Dillen, J.W. Geus, F.J.J.G. Janssen and F.M.G. Van der Kerkhof, J. Catal. 114 (1988) 313.
[19] W. Hua, Y. Xia, Y. Yue and Z. Gao, J. Catal. 196 (2000) 104.
[20] J.A. Moreno and G. Poncelet, J. Catal. 203 (2001) 153.
[21] J.R. Sohn and W.C. Park, Bull. Korean Chem. Soc. 21 (2000) 1063.
[22] J.R. Sohn and W.C. Park, Appl. Catal. A: Gen. 230 (2002) 11.
[23] J.R. Sohn, S.G. Cho, Y.I. Pae and S. Hayashi, J. Catal. 159 (1996) 170.
[24] J.R. Sohn, D.H. Seo and S.H. Lee, J. Ind. Eng. Chem. 10 (2004) 309.
[25] J.R. Sohn, J.G. Kim, T.D. Kwon and E.H. Park, Langmuir 18 (2002) 1666.
[26] O. Saur, M. Bensitel, A.B.M. Saad, J.C. Lavalley, J.C. Tripp and B.A. Morrow, J. Catal. 99 (1986) 104.
[27] T. Yamaguchi, Appl. Catal. 61 (1990) 1.
[28] T. Jin, T. Yamaguchi and K. Tananbe, J. Phys. Chem. 90 (1986) 4794.
[29] G. Cerrato, L. Marchese and C. Morterra, Appl. Surf. Sci. 70 (1993) 200.
[30] L.J. Alemany, F. Berti, G. Busca, G. Ramis, D. Robba, G.P. Toledo and M. Trombetta, Appl. Catal. B: Environ. 10 (1996) 299.
[31] J.R. Sohn and E.S. Cho, Appl. Catal. A:Gen. 282 (2005) 147.
[32] Y.I. Pae, M.H. Bae, W.C. Park and J.R. Sohn, Bull. Korean Chem. Soc. 25 (2004) 1881.
[33] J.R. Sohn and W.C. Park, Appl. Catal. A: Gen. 239 (2003) 269.
[34] R.V. Siriwardane, J.A. Poston Jr., E.P. Fisher, M.S. Shen and A.L. Miltz, Appl. Surf. Sci. 152 (1999) 219.
[35] J.R. Sohn, J. Ind. Eng. Chem. 10 (2004) 1.
[36] A. Satsuma, A. Hattori, K. Mizutani, A. Furuta, A. Miyamoto, T. Hattori and Y. Murakami, J. Phys. Chem. 92 (1988) 6052.
[37] S. J. Decanio, J. R. Sohn P. O. Fritz and J. H. Lunsford, 101 (1986) 132.
[38] K. Tanabe, *Solid Acids and Bases* (Kodansha, Tokyo, 1970) 103.
[39] J.R. Sohn and A. Ozaki, J. Catal. 61 (1980) 291.
[40] Y. Xia, W. Hua and Z. Gao, Appl. Catal. A: Gen. 185 (1999) 293.
[41] R.T. Sanderson, *Chemical Bonds and Bond Energy* (Academic Press, New York, 1976) 75.
[42] Z. Gao, Y. Xia, W. Hua and C. Miao, Topics Catal. 6 (1998) 101.